Reprinted From
Nonlinear Topics in Ocean Physics

Soc. Italiana di Fisica - Bologna - Italy

M. FARGE

Nonlinear Dynamics of Inertio-Gravity Waves

EDITRICE COMPOSITORI - BOLOGNA - 1991

Nonlinear Dynamics of Inertio-Gravity Waves.

M. FARGE
L.M.D.-C.N.R.S., Ecole Normale Supérieure - 24, rue Lhomond, 75231 Paris Cedex 5

1. – Introduction.

We study the nonlinear dynamics of a shallow-water layer in uniform rotation, which models the behaviour of large-scale atmospheric and oceanic flows. Its evolution is described by Saint-Venant equations, that we integrate numerically. We focus on the case of decaying turbulent flows dominated by divergent motions and subject to different rotation rates, in order to better understand the nonlinear dynamics of inertio-gravity waves.

2. – Saint-Venant equations.

Saint-Venant equations, also called shallow-water equations, describe the fluid motions in a rotating stratified shallow-water layer of depth h (fig. 1) and can be written in terms of the vorticity, divergence and geopotential time evolutions,

$$\xi_t + \operatorname{div}(\xi + f)\boldsymbol{V} = D\,,$$

$$\delta_t - \operatorname{rot}(\xi + f)\boldsymbol{V} + \Delta(\phi + V^2/2) = D\,,$$

$$\phi_t + \operatorname{div}(\phi \boldsymbol{V}) = D\,,$$

with $\phi = gh$, geopotential, $\boldsymbol{V}$, velocity, $\xi = \operatorname{rot} \boldsymbol{V}$, vorticity, $\delta = \operatorname{div} \boldsymbol{V}$, divergence, D, dissipation, f, Coriolis parameter, g, acceleration of gravity.

Due to stratification the equations have become two-dimensional.

The invariants of the inviscid Saint-Venant equations are energy

$$E = (1/2)\langle \phi^2 + \phi V^2 \rangle\,,$$

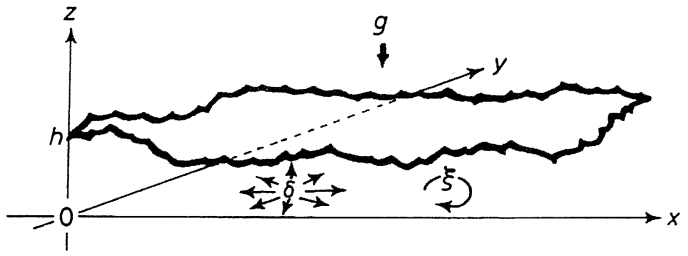

Fig. 1. – Rotating shallow-water layer.

$\langle\ \rangle$ means averaged over the plane, and potential enstrophy

$$S = (1/2)\,\langle(\xi + f)^2/\phi\rangle\,.$$

These invariants being nonquadratic, the modal energy decomposition is only possible if we consider the equations linearized around a rest state ($\delta = \xi = 0$ and $\phi = \overline{\phi}$):

$$\xi_t + f\delta = 0, \qquad \delta_t - f\xi + \Delta\phi = 0, \qquad \phi_t + \overline{\phi}\delta = 0\,.$$

These linearized equations then yield quadratic invariants, namely linearized energy

$$E = (1/2)\,\langle\phi^2 + \overline{\phi}V^2\rangle$$

and linearized potential enstropy

$$S' = (1/2)\,\langle\overline{\phi}\xi - f\phi\rangle.$$

The flow can now be separated into two classes of normal eigenmodes corresponding to

1) potential vortices (indexed V), which are nondivergent, stationary and contain all the linearized potential vorticity of the flow;

2) inertio-gravity waves (indexed G), which propagate with velocity $c = \overline{\phi}^{1/2}$, are dispersive in the presence of rotation, $\omega = (c^2k^2 + f^2)^{1/2}$, and contain all the divergent components of the flow.

We numerically solve the full Saint-Venant equations, using a pseudo-spectral technique for the space integration, associated to a leapfrog time scheme [1]. We choose different initial flows which are Gaussian random fields, whose energy is injected at $k_i = 3$ and which contain different levels of excitation of the divergence field, corresponding to the divergence energy which varies from 15% up to 99% of the total energy. We consider two different rotation rates, namely

$f = 10^{-4}$ s^{-1} and $f = 6 \cdot 10^{-4}$ s^{-1}, which correspond to a Rossby deformation wave number $k_d = f/c$ of, respectively, $k_d = 2$ and $k_d = 12$; the Rossby deformation radius $r_d = 2\pi/k_d$ gives the scale below which the flow becomes insensitive to the effect of the entrainment rotation. During the flow evolution there is no more energy injection. We, therefore, study the evolution of a decaying turbulent flow. The computing grid is 128^2, which corresponds to 64 Fourier modes $k = |\boldsymbol{k}|$, and we follow the flow evolution on very long time scales, of the order of several hundreds eddy turn-overs or 75 000 inertio-gravity wave periods.

3. – Inviscid statistical equilibria.

The natural tendency of an inviscid two-dimensional system, having a finite number of degrees of freedom and presenting a combination of rotational and divergent motions, is to accumulate potential enstrophy and inertio-gravitational energy in the small scales and potentio-vortical energy in the large scales [2, 3].

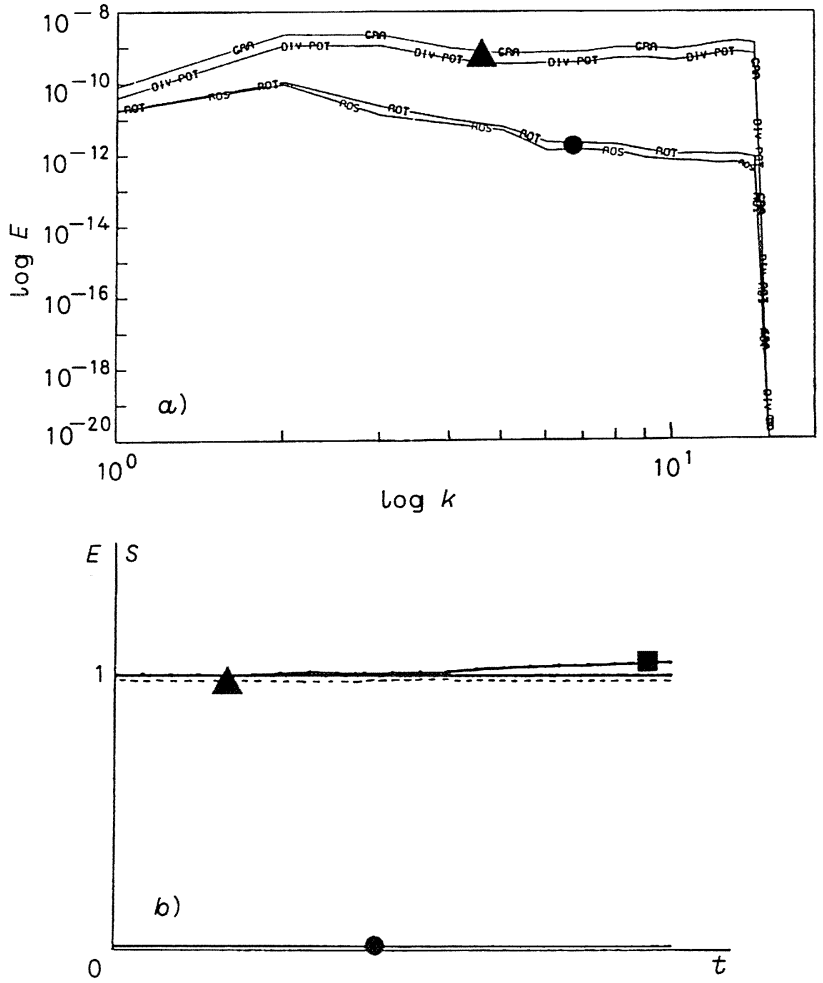

Fig. 2. – *a*) Energy spectra of the inviscid statistical equilibrium. (In all figures ● characterizes the energy of potential vortices, ▲ characterizes the energy of inertio-gravity waves, ■ characterizes the potential enstrophy of potential vortices.) *b*) Time evolution of energy and potential enstrophy.

This comes from the fact that the potential vortices behave as in the two-dimensional incompressible case, presenting an energy equipartition spectrum (k^{+1}) for $k \to 0$ and an enstrophy equipartition spectrum (k^{-1}) for $k \to k_{max}$. On the contrary, the inertio-gravity waves are not constrained by the potential enstrophy conservation, but only by the energy conservation, which leads then to an energy equipartition spectrum (k^{+1}) at all scales.

The numerical integration of the inviscid Saint-Venant equations gives the same spectra as those predicted (fig. 2*a*)) and confirms the good conservation properties of the chosen numerical scheme (fig. 2*b*)). Then, knowing the statistical equilibria, we can predict that, in the viscous case, there should be a dissipation of both potential enstrophy and inertio-gravitational energy, while the potentio-vortical energy should present an inverse cascade towards large scale where it would pile up.

The very different behaviours of potential vortices and inertio-gravity waves suggest that different parametrizations may be necessary depending on which component will dominate. The operator needed to model the subgrid-scale effects should indeed dissipate the potential enstrophy of potential vortices, as for two-dimensional incompressible flows, but also the divergence energy of inertio-gravity waves.

4. – Viscous behaviour.

As we have seen, we can separately study the potential vortex dynamics and the inertio-gravity wave dynamics if we are in the limit of weak geopotential fluctuations. Considering first the dynamics of potential vortices, its characteristic time corresponds to the rotational nonlinear transfers at scale k^{-1}, which can be evaluated from a root-mean-square measure of the velocity shears due to structures whose scale is larger than k^{-1}, *i.e.* from the kinetic enstrophy integral, such as

$$\tau'_V(k) \approx \left| \int p^4/(p^2 + k_d^2)\, E'(p)\, dp \right|^{-1/2},$$

with k_d the Rossby deformation wave number.

We can then calculate the potential enstrophy cascade rate, in the spectral range $k > k_d$ not affected by rotation, as

$$\eta \approx kS'(k)/\tau'_V(k).$$

This yields the same energy spectral distribution as for two-dimensional incompressible flows [4], namely,

$$E'_V(k) \approx \eta^{2/3} k^{-3}.$$

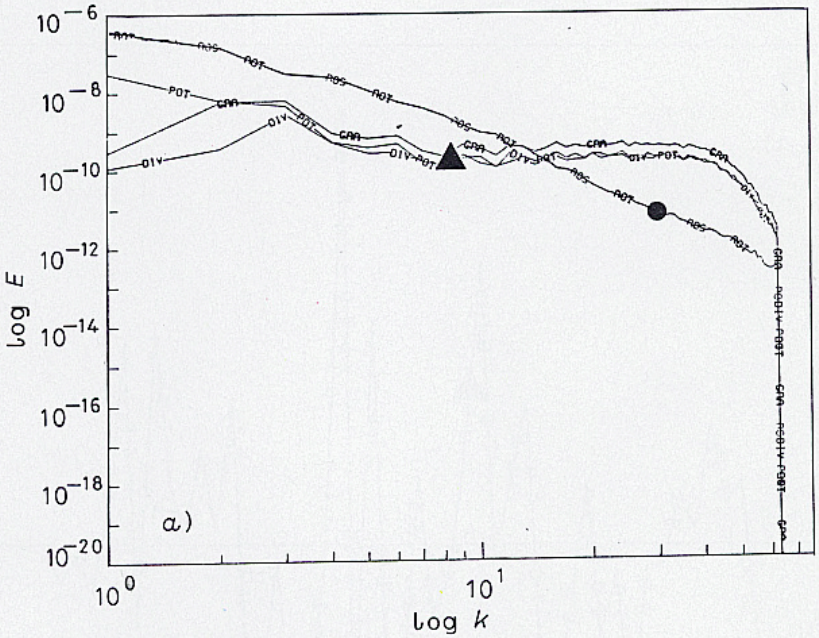

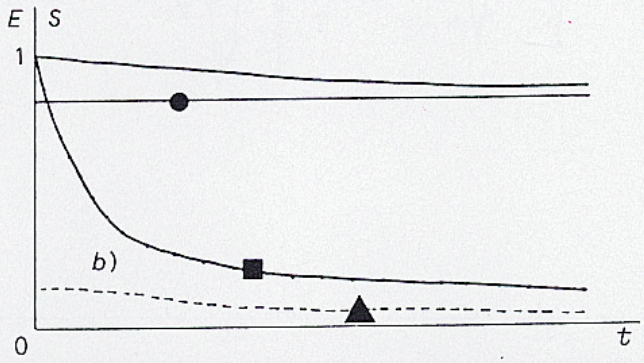

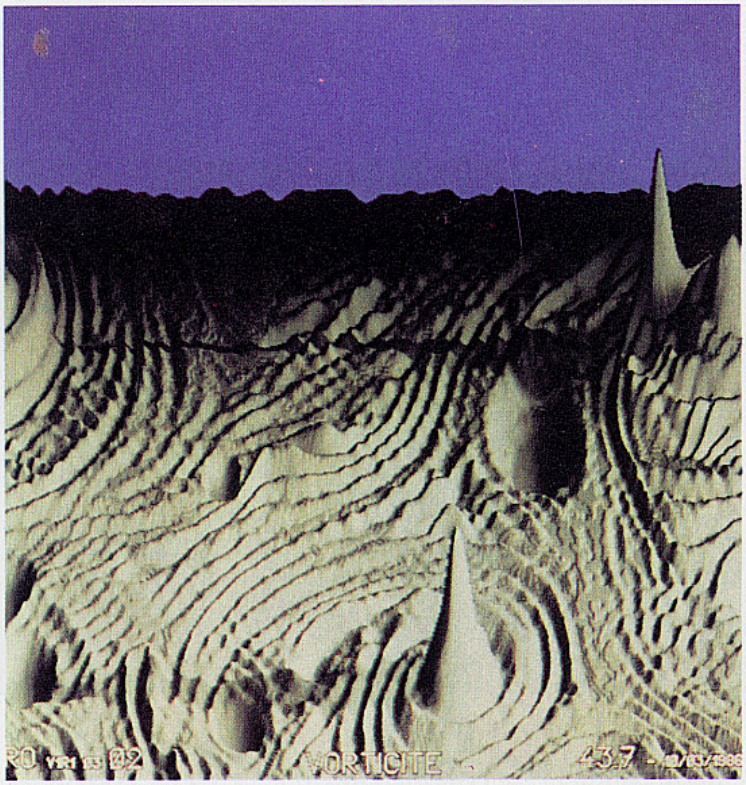

Fig. 3. – *a*) Energy spectra in the viscous case for a flow having initially 15% inertio-gravity waves and submitted to a slow rotation rate ($k_d = 2$). *b*) Time evolution of energy and potential enstrophy. *c*) Isolated coherent structures in the vorticity field.

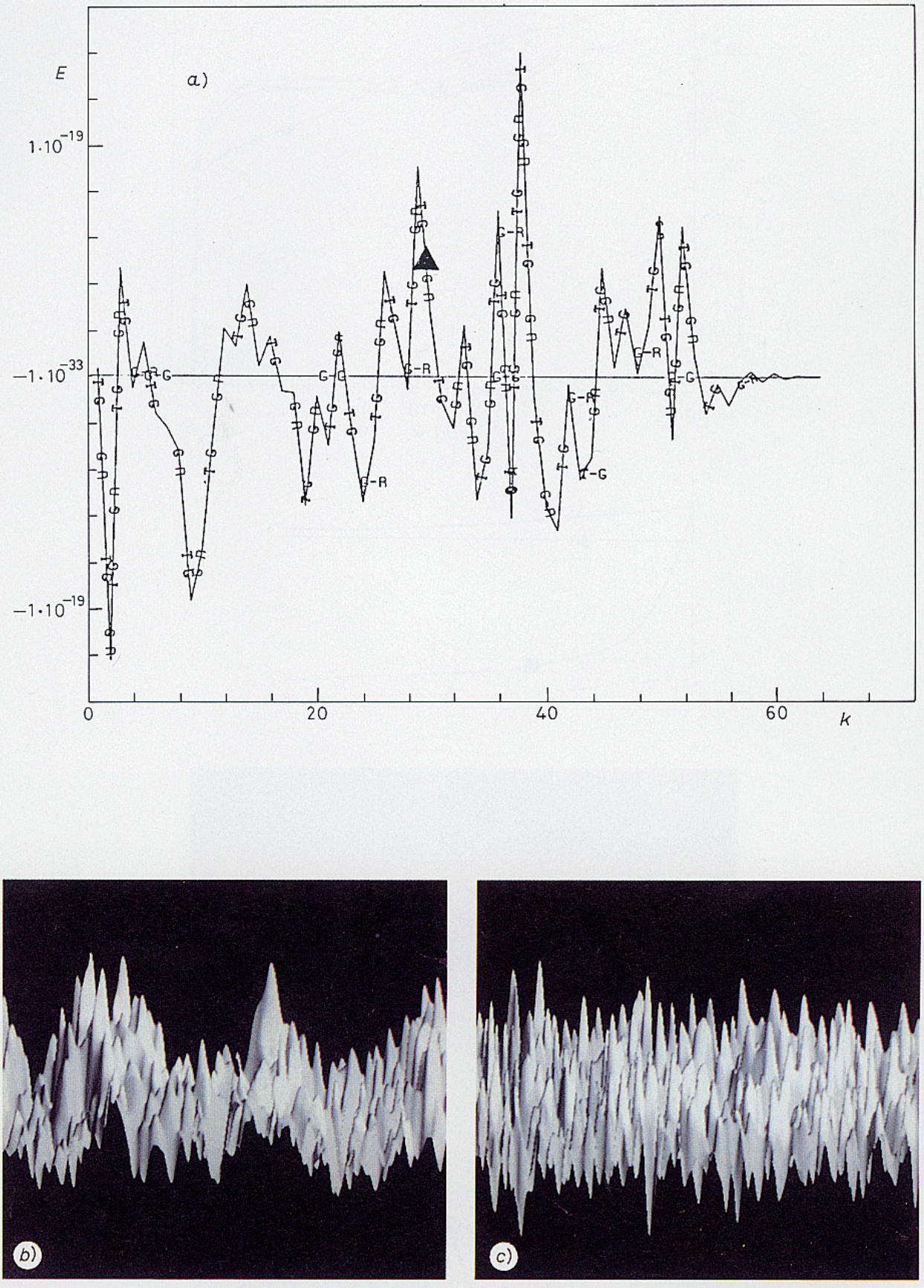

Fig. 4. – *a*) Quasi-instantaneous inertio-gravitational energy transfers for a flow having initially 99% inertio-gravity waves with slow rotation ($k_d = 2$). *b*) Inertio-gravity waves in the geopotential field. *c*) Inertio-gravity waves in the divergence field.

Considering now the dynamics of inertio-gravity waves, we can follow the same argument. If we suppose a transfer of divergence energy from the large to the small scales, its characteristic time corresponds to the transfers of divergence energy at scale k^{-1}, which can be evaluated from a root-mean-square measure of the gradients of divergent motions, such as

$$\tau'_{\mathrm{G}}(k) \approx \left| \int p^2 E'(p)\, \mathrm{d}p \right|^{-1/2}.$$

We can then calculate the divergence energy cascade rate:

$$\zeta \approx kE'(k)/\tau'_{\mathrm{G}}(k).$$

This yields a $k^{-5/3}$ spectral law of the energy distribution as for three-dimensional incompressible flows [5], namely,

$$E'_{\mathrm{G}}(k) \approx \zeta^{2/3} k^{-5/3}.$$

Using a different approach, ZAKHAROV and SAGDEEV [6] predict a $k^{-11/7}$ spectral law, namely a -1.57 slope instead of -1.66, for nondispersive two-dimensional acoustic turbulence, a problem which has a physics very similar to the nonlinear inertio-gravity wave dynamics studied here.

Concerning the energy of potential vortices, the numerical integrations for a flow having initially 15% inertio-gravity waves (fig. 3*a*)) show a k^{-4} power law spectrum. The rotational energy is piling up into the large scales, while the potential enstrophy is transferred towards the small scales where it is then dissipated (fig. 3*b*)). The transfer of potential enstrophy towards small scale is confirmed, but the slope of the rotational energy is steeper than the predicted k^{-3} tendency. This results from the spatial intermittency caused by the presence of coherent structures in the vorticity field (fig. 3*c*)): the transfers do not occur densely in space, but are concentrated in the boundary layers formed at the periphery of the coherent structures [7].

Concerning the energy of inertio-gravity waves for the same flow, which initially contains 15% inertio-gravity waves, we find a k^0 spectrum for the scales smaller than the injection scale k_{i} and larger than the dissipative scale k_{d} (fig. 3*a*)). We observe that the inertio-gravity wave energy reaches the small scales where it is dissipated (fig. 3*b*)), which explains the process of geostrophic adjustment in shallow-water flow, *i.e.* the dominance of potential vortices over inertio-gravity waves which ultimately disappear. The observed k^0 spectrum, steeper than an equipartition spectrum (k^{+1}), is probably related to the shape of the shocks which would develop in the absence of dissipation. Indeed, the shallow-water model, contrary to the Korteweg-deVries model, is not dispersive and, therefore, produces shocks which tend to break. This wave breaking, possible in the absence of dissipation, is easy to understand if we consider the

simple case of a wave propagating with amplitude h' in a shallow fluid layer of mean depth H. The wave trough travels with the group velocity $v_t = (gH)^{1/2}$, while the wave ridge travels with the velocity $v_r = (g(H + h'))^{1/2}$. Therefore, the ridge moves faster than the trough and, consequently, must eventually break. In fact, this behaviour is not realistic, because in an actual fluid the shocks will get dispersed (as for the Korteweg-deVries model) through the emission of capillary ripples, which then will limit the process of wave breaking. But in the shallow-water model the dissipation may play the same role as dispersion in damping the strong geopotential gradients before shocks get formed and eventually break.

It is important to notice that we are still in the domain of validity of the shallow-water hypothesis, because the smallest spatial scales considered here remain 10 times larger than the water depth, and the vertical velocities are negligible, although their gradients may be strong.

The quasi-instantaneous transfers (fig. 4*a*)) for a flow having initially 99% inertio-gravity waves show that the divergence energy is transferred back and forth with no overall direction: waves do not seem to cascade, divergence energy being only dissipated (fig. 5*b*)) when, by chance, some wave interactions bring

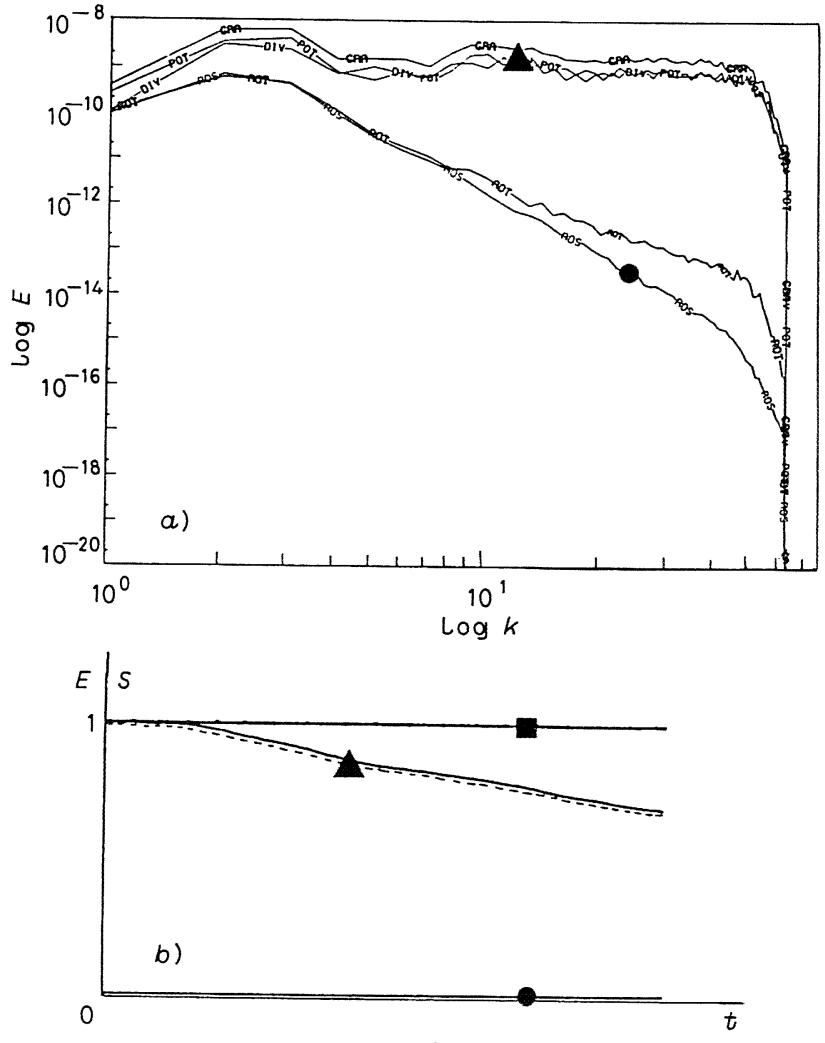

Fig. 5. – *a*) Energy spectra in the viscous case for a slow rotation rate ($k_d = 2$) with a rotational turbulent viscosity only. *b*) Time evolution of energy and potential enstrophy.

energy into the small scales. The prediction done on phenomenological grounds, leading to a $k^{-5/3}$ spectral slope, close to the $k^{-7/11}$ slope predicted by ZAKHAROV and SAGDEEV [6], is not verified, because it is based on the hypothesis of an overall energy cascade towards small scales that we do not actually observe.

The k^0 spectrum we again obtain in this case (fig. 5*a*) and 6*a*)) can be interpreted in terms of the shape of the singularities which tend to develop in this shallow-water flow. By visualizing in physical space the fields corresponding to the inertio-gravity waves, namely the geopotential (fig. 4*a*)) and divergence (fig. 4*b*)) fields, we observe the formation of spikelike features. As a first approximation we consider them to be axisymmetric and we suppose a radial shape such as $f(r) = r^\beta e^{-r}$, r being the distance from the centre of the spike and β a real exponent. From there we calculate that the two-dimensional energy spectrum should vary as

$$E(|\boldsymbol{k}|) \propto |\boldsymbol{k}|^{-2\beta-4}.$$

Considering the fact that we experimentally observe a k^0 spectrum, we can predict that $\beta = -2$, which would correspond to a singularity such as $f(r) = r^{-2} e^{-r}$, if dissipation would not have been there to smooth it.

5. – Subgrid-scale parametrization.

We have tested different subgrid-scale parametrizations designed to dissipate both potential enstrophy and inertio-gravity wave energy in the small scales. In all cases we choose the hyperdissipation operator Δ^α, with $\alpha > 1$, which is commonly used and has proven its adequacy in the context of two-dimensional turbulence [7]. We consider here $\alpha = 8$, which gives an hyperdissipation highly selective in scales, that we apply to all fields, namely to the vorticity, divergence and geopotential fields. In the shallow-water model the geopotential dissipation is needed for physical reasons, because a strong geopotential gradient corresponds indeed to a strong gradient of vertical velocity, which has to be dissipated too. Therefore, we dissipate the geopotential, *i.e.* the free-surface height, in order to control the vertical velocity gradients and the process of wave breaking.

We have tested three different kinds of subgrid-scale parametrization that we apply at each time step to selectively damp the enstrophy of the potential vortices and the energy of the inertio-gravity waves, which both cascade towards the small scales where they are dissipated.

1) The first parametrization (fig. 5*a*) and *b*)) dissipates the potential vortices and the waves with the same $\nu\Delta^8$ operator and the viscosity ν is adjusted on the rotational motions only (ν_R being then called the «rotational turbulent viscosity»), *i.e.* on the transfer rate of kinetic enstrophy through the cut-off scale

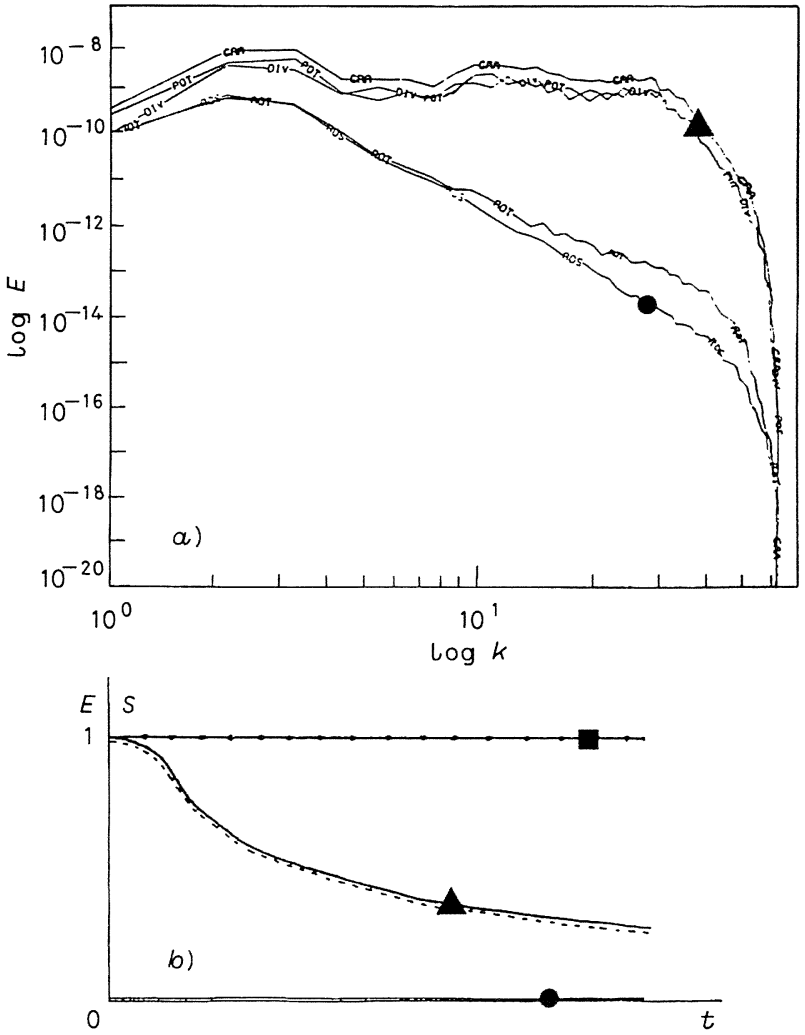

Fig. 6. – *a*) Energy spectra in the viscous case for a slow rotation rate ($k_d = 2$) with both rotational and divergent turbulent viscosity. *b*) Time evolution of energy and potential enstrophy.

k_c, such as

$$\nu_R = k_c^{16} \langle \xi^2 \rangle^{1/2}.$$

2) The second parametrization (fig. 6*a*) and *b*)) again dissipates the potential vortices and the waves with the same $\nu\Delta^8$ operator, but now the viscosity ν is adjusted on both rotational and divergent motions, *i.e.* taking also into acount the transfer rate of divergence energy through the cut-off scale k_c, such as

$$\nu = \max|\nu_R, \nu_D|,$$

with $\nu_D = k_c^{16} \langle \delta^2 \rangle^{1/2}$, ν_D being then called the «divergence turbulent viscosity».

3) The third parametrization is designed to selectively dissipate the inertio-gravity waves with an Asselin's frequency filter [8] such as

$$|X^n|_{\text{filtered}} = X^n + \varepsilon (X^{n-1} - 2X^n + X^{n+1}.$$

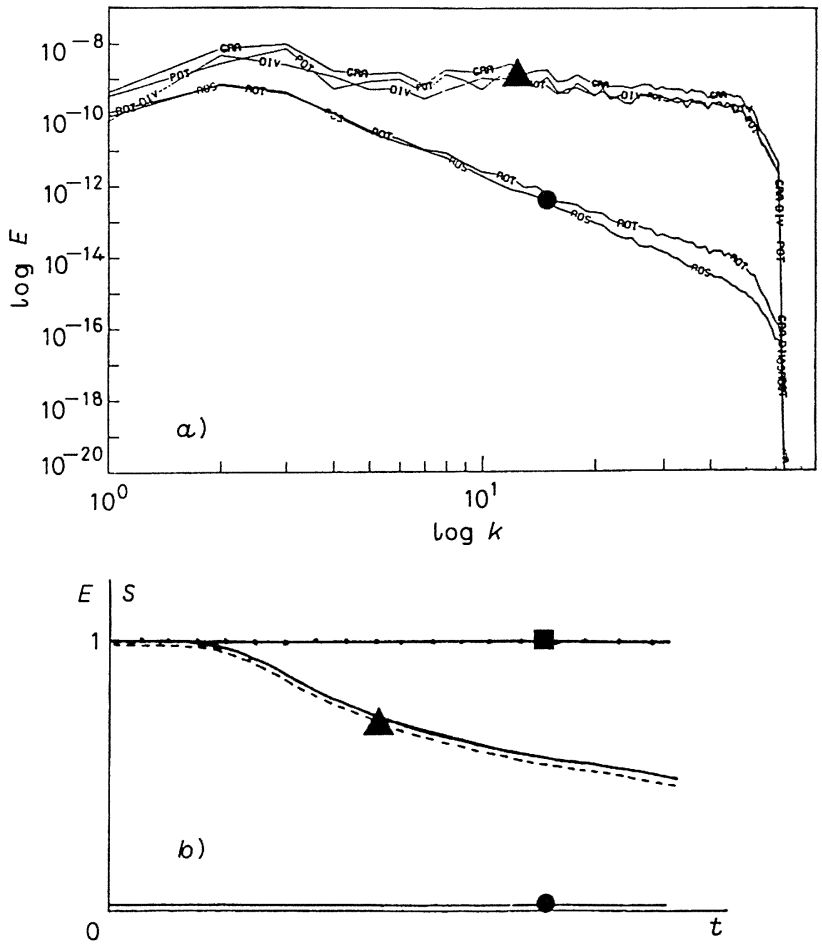

Fig. 7. – *a*) Energy spectra in the viscous case for a slow rotation rate ($k_d = 2$) with an Asselin's filter with $\varepsilon = 10^{-4}$. *b*) Time evolution of energy and potential enstrophy.

$\boldsymbol{X}$ vector field at time step n, considering different damping ε. Actually this filter, which is a time Laplacian, also acts as a space Laplacian $\varepsilon\Delta^2$ in the small scales, because there the waves are nondispersive, being insensitive to rotation for wave numbers larger than the Rossby deformation wave number k_d. The damping $\varepsilon = 10^{-4}$ (fig. 7*a*) and *b*)) appears to be too weak to dissipate the waves more than the $\nu\Delta^8$ operator; on the contrary, $\varepsilon = 10^{-2}$ (fig. 9*a*) and *b*)) strongly damps the waves until the very large scales close to $k_i = 3$, while $\varepsilon = 10^{-3}$ (fig. 8*a*) and *b*)) damps the waves only in the small scales beyond $k = 30$, which seems more adequate. It is important to notice that, whatever is ε, the Asselin's filter does not affect the potential vortices whose behaviour remains unchanged.

In conclusion, we choose the second parametrization as the most appropriate, because it does not require any *ad hoc* parameter, as the ε damping of the Asselin's filter, and it takes into account the cascade of both kinetic enstrophy and divergence energy towards the small scales, while the first parametrization neglects the transfers of divergent motions. We notice that the tendency towards a k^0 spectrum for the inertio-gravity energy survives whatever parametrization we choose; this should be thought as a very basic behaviour of

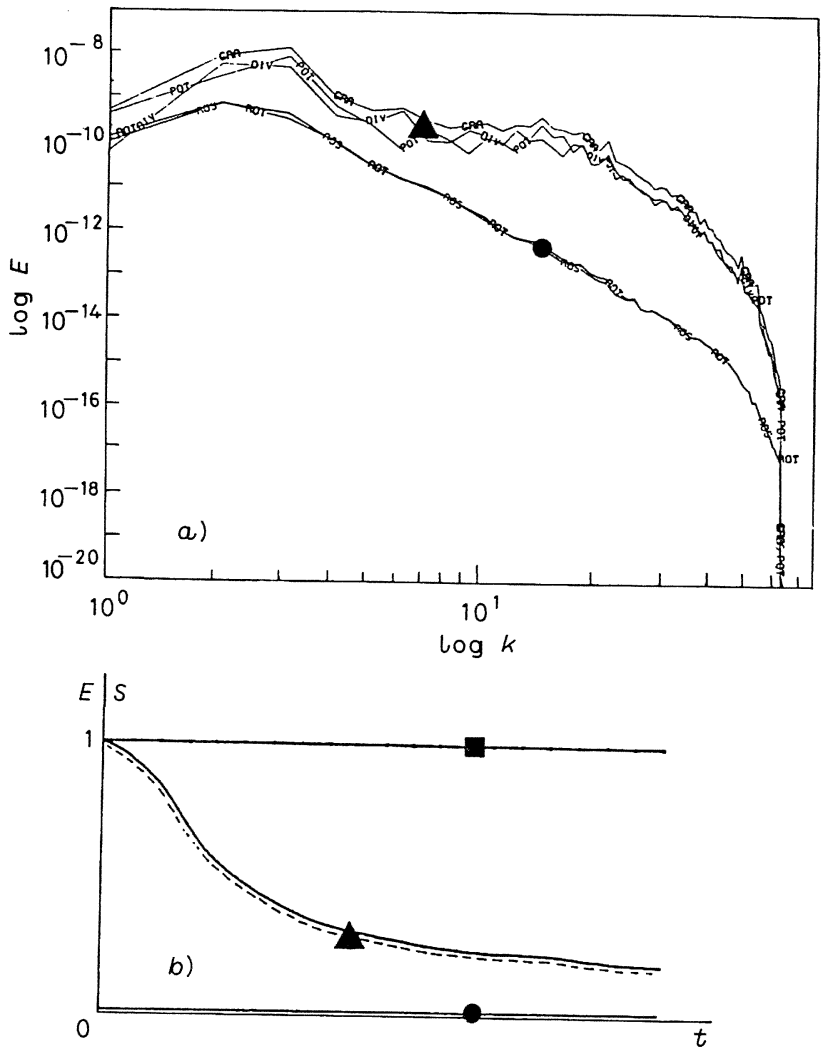

Fig. 8. – *a*) Energy spectra in the viscous case for a slow rotation rate ($k_d = 2$) with an Asselin's filter with $\varepsilon = 10^{-3}$. *b*) Time evolution of energy and potential enstrophy.

the shallow-water dynamics and not as a numerical artifact depending on the subgrid-scale parametrization.

6. – Effect of rotation.

The experiments discussed in sect. 4 and 5 correspond to a slow rotation rate, $f = 10^{-4}$ s^{-1} or $k_d = 2$, therefore all the scales in the inertial range, corresponding to wave numbers between $k_i = 3$ and $k_c = 64$, are insensitive to rotation, because in this case $k_i > k_d$. We now consider a higher rotation rate, namely $f = 6 \cdot 10^{-4}$ s^{-1}, corresponding to $k_d = 12$, for which the large scales, in the range between $k_i = 3$ and $k_d = 12$, are then submitted to the effect of rotation.

If we first consider the dynamics of potential vortices, we observe that the rotation reduces both the direct potential enstrophy cascade and the inverse rotational-energy cascade (fig. 10*a*)). This comes from the fact that the potential enstrophy S separates into a kinetic contribution S_{kin} and a potential contribution

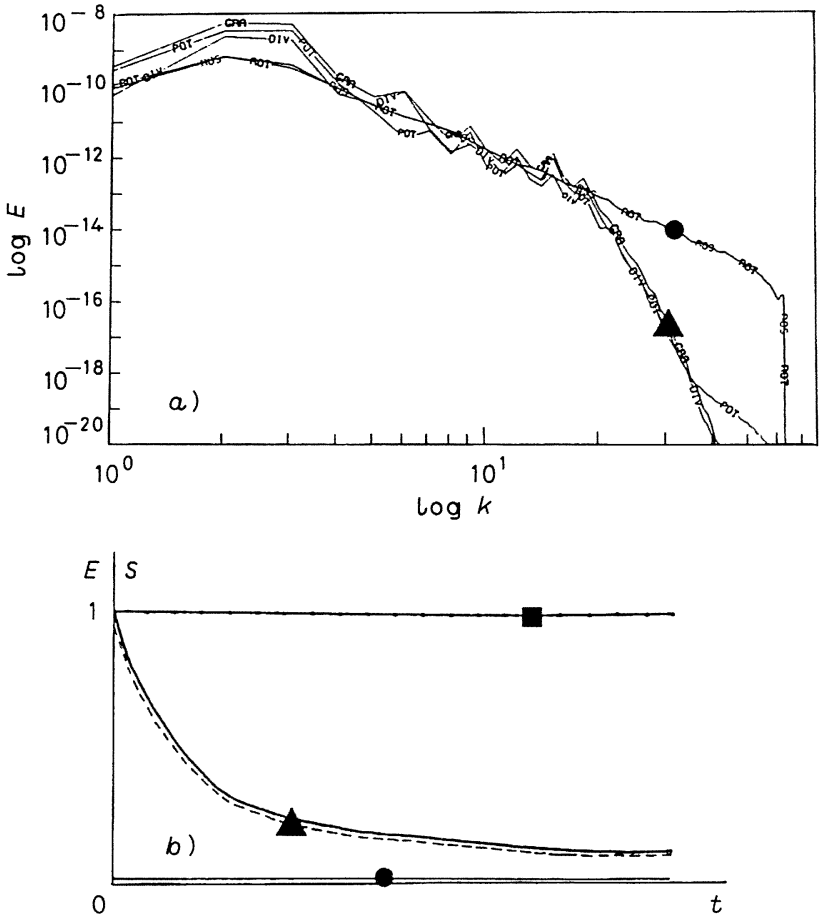

Fig. 9. – *a*) Energy spectra in the viscous case for a slow rotation rate ($k_d = 2$) with an Asselin's filter with $\varepsilon = 10^{-2}$. *b*) Time evolution of energy and potential enstrophy.

S_{pot}, such as

$$S = (c/2) \int (k^2 + k_d^2) E_V(k) \, dk = S_{kin} + S_{pot}$$

with $E_V(k)$ rotational energy of each potential vortical mode,

$$S_{kin} = (c/2) \int k^2 E_V(k) \, dk$$

and

$$S_{pot} = (c/2) \int k_d^2 E_V(k) \, dk .$$

Therefore, when k_d is large, *i.e.* for strong rotation rates, most of enstrophy is potential and stays in the large scales, while only the remaining amount, which is kinetic, cascades towards the small scales: both this direct enstrophy cascade and the associated inverse rotational-energy cascade are weakened under the effect of rotation. This can also be observed on the structure of the vorticity field in physical space (fig. 10*c*)): the vortices are no longer isolated and we do not see any background flow of vorticity filaments produced by the direct enstrophy cascade as it is the case when rotation is small (fig. 3*c*)).

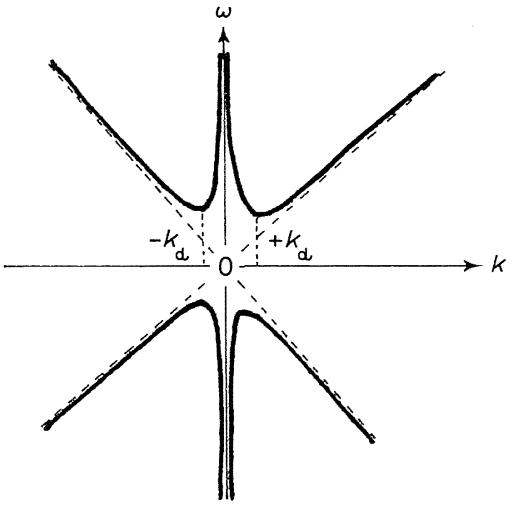

Fig. 11. – Dispersion diagram of inertio-gravity waves in a rotating shallow-water layer.

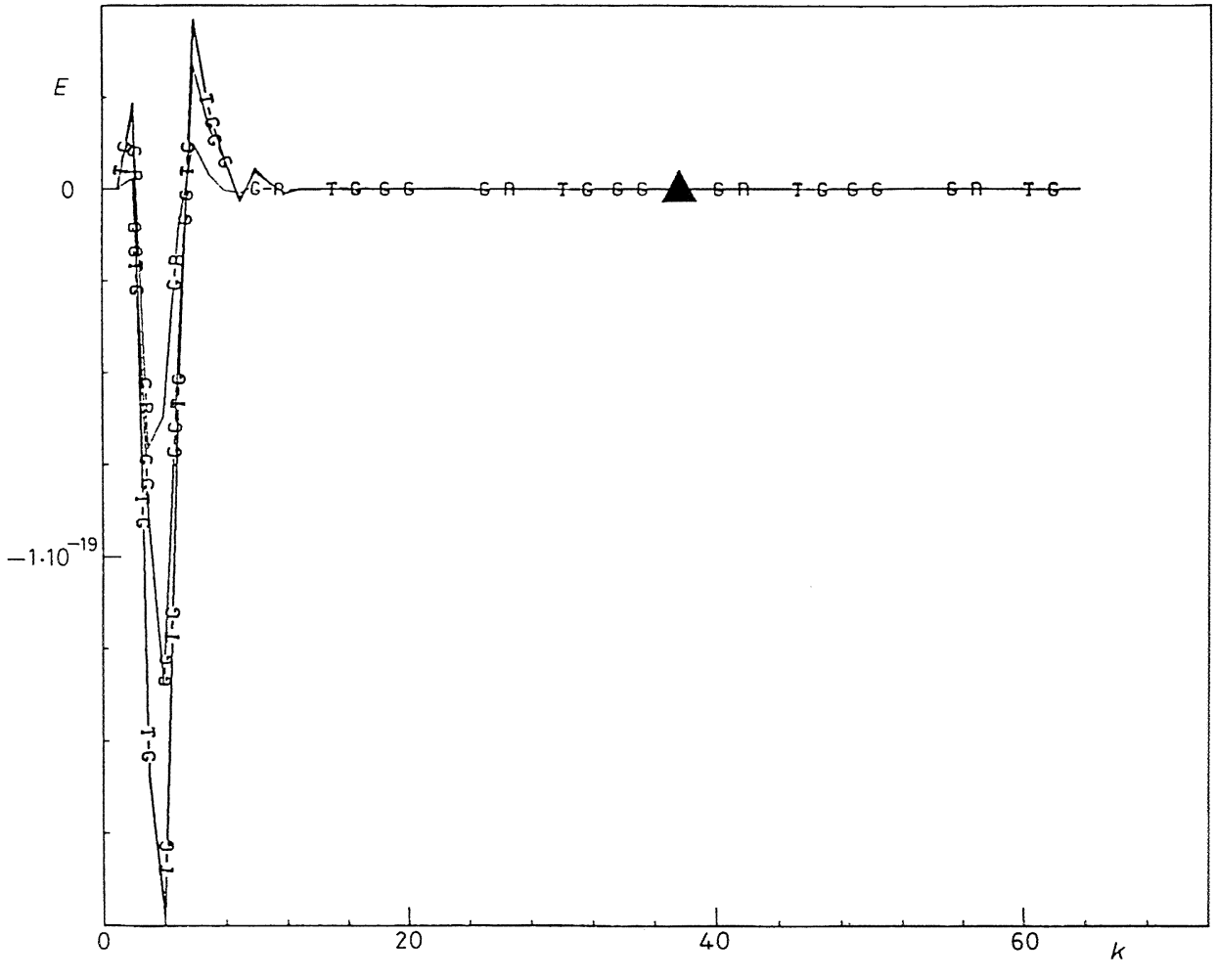

Fig. 12. – Quasi-instantaneous inertio-gravitational energy transfers for a flow having initially 75% inertio-gravity waves submitted to a fast rotation rate ($k_d = 12$).

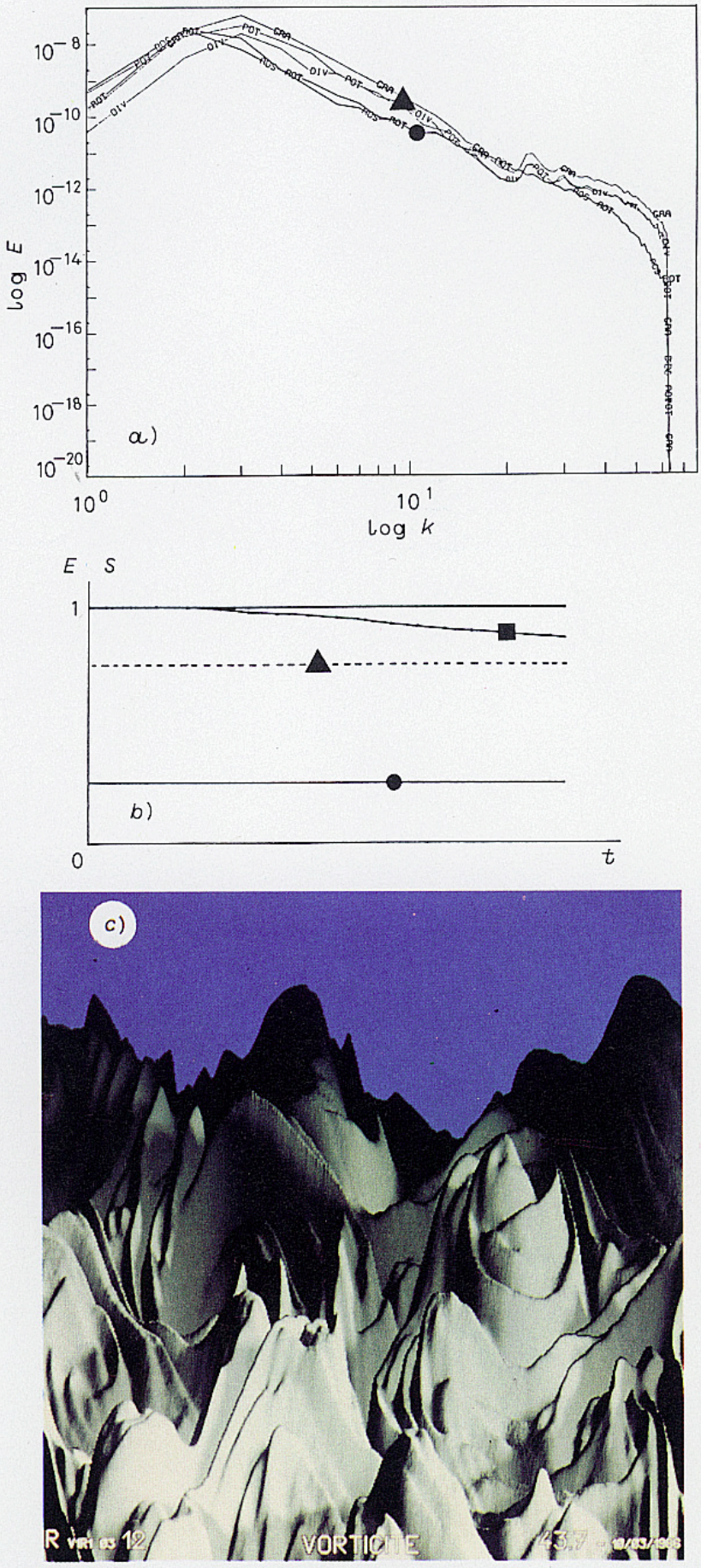

Fig. 10. – *a*) Energy spectra in the viscous case for a flow having 75% inertio-gravity waves initially submitted to a fast rotation rate ($k_d = 12$). *b*) Time evolution of energy and potential enstrophy. *c*) Nonisolated coherent structures in the vorticity field.

If we now consider the dynamics of inertio-gravity waves, we observe that the rotation strongly inhibits the transfers of inertio-gravity energy towards the small scales and the related dissipation (fig. 10*b*)), while the corresponding spectrum stays frozen close to its initial distribution (fig. 10*a*)). This is readily explained by looking at the dispersion law (fig. 11):

$$\omega = (ck^2 + f^2)^{1/2} = c(k^2 + k_d^2)^{1/2} \sim c\,(k + k_d^2/2k)\,,$$

with ω the inertio-gravity wave frequency, which shows that waves $|\boldsymbol{k}| < k_d$ are dispersive, they cannot have triadic interactions but only quartic, and, therefore, the nonlinear transfers (fig. 12) between those wave modes are strongly reduced under the effect of rotation: no more energy is feeding the small scales and there is no dissipation of inertio-gravitational energy. In consequence, if rotation is strong enough, namely if $k_d > k_i$, there is no more geostrophic adjustment, the inertio-gravity waves cannot be dissipated because they remain trapped in the large scales.

7. – Conclusion.

The nonlinear dynamics of inertio-gravity waves remains an open question, because we do not have a criterium to decide if the 64 modes we have integrated are sufficient to correctly describe the system evolution. We numerically predict that all scales are active, inertio-gravitational energy being transferred back and forth at random but without presenting an overall cascade and is distributed according to a k^0 spectrum. This nonlinear behaviour of two-dimensional shallow-water equations can be compared to the behaviour of the two-dimensional Schrödinger equation, which also tends to spread energy into higher and higher modes. In the absence of a predominant direction of transfers, it will be very difficult to develop a statistical theory of the nonlinear inertio-gravity wave motions, as has been done for turbulent motions. In consequence, the subgrid-scale parametrization may be difficult to ascertain if the small scales are not slaved by the large-scale dynamics feeding them. A better theoretical insight is needed here, because this behaviour may impair the numerical approach in this case, the nonlinear inertio-gravity wave dynamics appearing resolution dependent due to the k^0 spectral tendency we observe.

* * *

The computing has been done on the Cray 2 of C2VR, Palaiseau, using as front-end the IBM 3090 of CIRCE, Orsay. High-resolution raster displays have been done at LACTAMME, Ecole Polytechnique, in collaboration with J.-F. COLONNA.

REFERENCES

[1] M. FARGE and J. F. LACARRA: *J. Int. Méc. Théor. Appl.*, Suppl. No. 2, **7**, 63 (1988).
[2] M. FARGE: *Statistical equilibria of divergent two-dimensional flows*, in *8th Symposium on «Turbulence and Diffusion», San Diego* (American Meteorological Society, 1988).
[3] M. FARGE and R. SADOURNY: *J. Fluid Mech.*, **206**, 433 (1989).
[4] R. H. KRAICHNAN: *Phys. Fluids*, **10**, 1417 (1967).
[5] A. M. KOLMOGOROV: *Isv. Akad. Nauk SSSR*, **31**, 538 (1941).
[6] V. E. ZAKHAROV and R. Z. SAGDEEV: *Sov. Phys. Dokl.*, **15**, 439 (1970).
[7] J. MCWILLIAMS: *J. Fluid Mech.*, **146**, 21 (1984).
[8] R. ASSELI.: *Mon. Weather Rev.*, **100**, 487 (1972).